This is an open access article published under a Creative Commons Non-Commercial No Derivative Works (CC-BY-NC-ND) Attribution License, which permits copying and redistribution of the article, and creation of adaptations, all for non-commercial purposes.

THE JOURNAL OF PHYSICAL CHEMISTRY C

Article

Cite This: J. Phys. Chem. C XXXX, XXX, XXX−XXX

pubs.acs.org/JPCC

Time-Dependent Photoluminescence of Nanostructured Anatase TiO_2 and the Role of Bulk and Surface Processes

Robert Brüninghoff,[†] Kasper Wenderich,[†] Jeroen P. Korterik,[‡] Bastian T. Mei,[†] Guido Mul,[†] and Annemarie Huijser*[,†]

[†]MESA+ Institute, Photocatalytic Synthesis Group, University of Twente, P.O. Box 217, 7500 AE Enschede, The Netherlands

[‡]MESA+ Institute, Optical Sciences Group, University of Twente, P.O. Box 217, 7500 AE Enschede, The Netherlands

Supporting Information

ABSTRACT: TiO_2 is one of the most attractive photocatalysts, with applications in water splitting, wastewater treatment, and air purification. Understanding the fundamentals of the functioning of TiO_2 requires knowledge of the nature and dynamics of photo-induced excitons and charge carriers. Although photoluminescence (PL) spectroscopy can provide important fundamental insights, photophysical mechanisms are still under debate. To address this problem, the aim of the present work is to investigate the evolution of the PL spectrum in time of nanostructured anatase TiO_2 thin films and the nature of associated processes, at room temperature and in aqueous media closely resembling photocatalytic conditions. We show that the PL spectrum of commonly used nanostructured anatase TiO_2 thin films in aqueous media is time-dependent, with pH-dependent broadening at the low energy side of the spectrum in time. By global analysis of the spectrotemporal PL behavior and the effect of addition of NaCl at neutral and mildly acidic conditions, we show that this spectral development is due to an increasing contribution of processes sensitive to surface termination relative to bulk processes to the PL in time. The time-dependent PL spectrum and dynamics can be assigned to the recombination of mobile electrons populating the conduction band or shallow traps with immobile hole polarons in deep traps and motion of electrons from the nanoparticle bulk toward the depletion layer/surface in ca. 1 ns. This directionality likely plays an important role in the photocatalytic performance of nanostructured anatase TiO_2 and effects of ions such as chloride in aqueous media. Control of the directional motion of electrons and suppression of surface charge recombination via surface engineering show promise to further increase the photocatalytic activity.

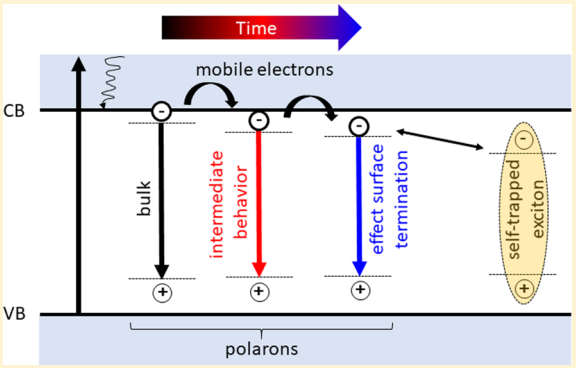

INTRODUCTION

TiO_2 is one of the most popular and often studied photocatalytic materials because of its abundance, nontoxicity, stability, and low cost,[1,2] with applications in amongst others photo(electro)chemical water splitting, wastewater treatment, and air purification.[3,4] Three polymorphs of TiO_2 are known: rutile, anatase, and brookite,[3] of which rutile and anatase are the most studied.[3,5] Rutile is the thermodynamically most stable form of TiO_2 and has a direct, forbidden band gap of 3.0 eV, while an indirect band gap of 3.2 eV is characteristic for the metastable anatase phase.[3,6] Anatase is proposed to have better photocatalytic properties than rutile because of a higher Fermi level and possibly a higher surface hydroxylation rate.[2,6] Furthermore, faster recombination of electrons and holes in rutile compared to anatase has been reported.[7] Photo-induced charge carriers can be used for photocatalytic reactions, provided they have a sufficiently long lifetime and are able to diffuse to the surface of the photocatalyst. Hence, understanding of the localization of photo-induced charge carriers and the development in time is important. The mobility of holes is thought to be the limiting step.[2,6,7] To overcome this, a high surface-to-volume ratio can be utilized to increase the photocatalytic activity.[2] Such ratio can be realized by the use of small nanoparticles of TiO_2, for instance, in a nanostructured film.[2,8−10]

The photo-induced mechanisms and dynamics in TiO_2 are still not fully understood.[2,6,11,12] Spectroscopic techniques are powerful to elucidate the nature of photogenerated excitons and charge carriers and their role in photocatalytic processes. Examples of spectroscopic techniques used to study TiO_2 include, but are not limited to, transient absorption,[6,13−16] frequency- and time-resolved microwave conductance,[6,17−19] sum-frequency generation vibrational spectroscopy,[20] and ultrafast two-dimensional deep-ultraviolet spectroscopy.[21] Moreover, photoluminescence (PL) spectroscopy is a powerful tool to unravel the photodynamics and discriminate between processes sensitive to surface termination and bulk processes.

Received: July 19, 2019
Revised: October 3, 2019
Published: October 11, 2019

Downloaded via UNIV TWENTE on October 24, 2019 at 11:56:19 (UTC).
See https://pubs.acs.org/sharingguidelines for options on how to legitimately share published articles.

DOI: 10.1021/acs.jpcc.9b06890
J. Phys. Chem. C XXXX, XXX, XXX−XXX

A variety of PL mechanisms have been reported.[2,11,22,23] One theory is that PL is linked to self-trapped excitons (STEs).[24−26] Besides STEs, PL has been proposed to result from radiative electron−hole combination at chemical defects,[10,11,27] a combination of both STEs and defects[23,28] or from donor−acceptor recombination (with oxygen vacancies and hydroxyl groups mainly acting as donor and acceptor sites, respectively).[29] Photogenerated electrons and holes can become trapped in bulk, sub-surface, or surface defects, typically assigned to oxygen vacancies, Ti^{3+} sites, O^- centers, and surface hydroxide species.[9−11,30−32] In addition, charge−phonon coupling could lead to polaron formation.[33−36] The indirect band gap results in a very weak and thermally activated PL for which phonon assistance is required.[2,9,25,37,38] Besides these different mechanisms for PL, the PL intensity and spectrum have been shown to be strongly dependent on the chemical environment,[9,11,23,39] indicating a major role of surface adsorbates potentially introducing new photochemical decay pathways or changing band bending.[40,41] Other factors influencing the spectral shape include the morphology of the TiO_2 nanoparticles,[10,39] the temperature,[23,42] and the chemical or thermal surface treatment influencing the number of surface defects.[8,43,44] In addition, interference effects leading to Fabry−Perot fringes have been observed for anatase films with high homogeneity and optical quality.[11] These studies illustrate that PL in TiO_2 is complex and the photophysical mechanisms are still under debate.

Recent work by Pallotti et al. discriminates between two main contributions to the PL of nanostructured anatase TiO_2 films: a "green" component around 2.3−2.5 eV (495−540 nm) attributed to the presence of surface oxygen vacancies and a "red" component around 1.9−2.1 eV (600−650 nm) assigned to subsurface oxygen vacancies.[11] The green PL is ascribed to radiative recombination of mobile electrons in the conduction band (CB) or shallow bulk traps with immobile holes trapped in deep defect states [0.7−1.4 eV above the valence band (VB) edge]. Similarly, red PL is assigned to radiative recombination of electrons in deep traps (0.7−1.6 eV below the CB edge) with mobile holes in the VB.

Apart from steady-state PL, a few authors have performed time-resolved PL experiments to resolve the lifetime of photogenerated electrons and holes.[6,23,45−47] Yamada and Kanemitsu demonstrated for anatase TiO_2 single crystals nonexponential decay profiles and considerably shorter lifetimes for holes (in the order of nanoseconds) compared to electrons (in the order of microseconds), with the diffusion of the latter proposed to occur through multiple-trapping-dominated transport via shallow trap states.[6] In a PL study at a low temperature (12 K), Cavigli et al. demonstrated for anatase TiO_2 nanoparticles both bulk and surface recombination, with the first only observable in the first 100 ps after excitation.[23] A fast and a slow component were correlated to direct and indirect formation of STEs, with the latter driven by quasi-free carriers. Dozzi and co-workers detected three lifetimes in their time-resolved PL decays of powder pellets of F-doped anatase TiO_2, in the order of tens, hundreds, and thousands of picoseconds.[45] The two fastest components were ascribed to exciton recombination, while the third most intense component was attributed to surface processes.

The aim of this work is to investigate the evolution of the PL spectrum in time of nanostructured anatase TiO_2 thin films and the nature of associated processes, at room temperature and in various aqueous media closely resembling photocatalytic conditions.[48,49] This enables us, to the best of our knowledge for the first time, to perform global analysis of spectrotemporal developments observed and to determine the decay-associated spectra (DAS). A key advantage of global and target analysis of time-resolved spectra is the discrimination of all the features giving rise to the signal, regardless of spectral overlap.[50] The experiments have been performed in a low photo-excitation intensity regime where the PL signal scales linearly with the number of incident photons.

To mimic various photocatalytic conditions and changes in pH during a reaction,[51] we have performed experiments in neutral and mildly acidic conditions both in the absence and presence of NaCl. Industrial wastewater typically contains significant levels of NaCl, which negatively affects activity in photocatalytic oxidation of aqueous hydrocarbons.[51] The pH has been tuned to be between values of 6.5 and 3.3 to control the surface charge and enable surface adsorption of either Na^+ or Cl^- ions (the point of zero charge of TiO_2 is around 6).[52] We demonstrate that the PL spectrum is time-dependent, with the intensity ratio of the low energy component relative to the higher energy component increasing with time. Furthermore, we show that the ps−ns dynamics and spectral changes can be assigned to motion of electrons from the nanoparticle bulk in the direction of the depletion layer/surface in ca. 1 ns. As a result, the effect of surface termination on the PL increases with time. This directionality in electron diffusion is vital for photocatalytic surface reactions and likely plays an important role in the photocatalytic performance of nanostructured anatase TiO_2. Suppression of charge recombination by surface engineering hence shows promise to improve the photocatalytic activity.

EXPERIMENTAL METHODS

Chemicals and Materials. The following chemicals and materials were used for sample preparation and experiments: methanol (≥99.9% Ultra for LC−MS, VWR), sodium chloride (99.7%, Sigma-Aldrich), demineralized water (Merck Milli-Q system, resistivity > 18 MΩ cm, pH ≈ 7), HNO_3 (ACS reagent, 70%, Sigma-Aldrich), and TiO_2 [Hombikat UV 100, Sachtleben (Venator)]; UV fused silica substrates (Suprasil 2000, 12 mm × 30 mm × 1 mm, UQG optics Ltd. UK) and fluorescence quartz cuvette (101-QS, Hellma Analytics; 10 mm × 10 mm optical path length).

Sample Preparation and Characterization. The UV fused silica substrates were cleaned by ultrasonication in acetone and afterward in water, rinsed with water, and dried under N_2 flow. In previous studies, we have demonstrated that sufficient calcination (≥600 °C) in air of anatase TiO_2 [Hombikat UV 100, Sachtleben (Venator)] yields an increase in photocatalytic activity.[53,54] Before film preparation, the TiO_2 powder was therefore annealed at 600 °C in air, followed by suspension of ca. 50 mg of TiO_2 powder in 5 mL of methanol or water and ultrasonication for 30 min. The nanostructured TiO_2 films were prepared by drop-casting the TiO_2 suspension on the cleaned silica substrates followed by drying at 80 °C, resulting in homogeneous semi-translucent films in case methanol was used. The use of water-based suspensions led to less homogeneous coatings. X-ray diffraction patterns were recorded using a D2 PHASER X-ray powder diffractometer (Bruker) using the Cu Kα line under an acceleration voltage of 30 kV. Scanning electron microscopy (SEM) images were recorded at the MESA+ NanoLab facility using a Zeiss Merlin HR-SEM.

DOI: 10.1021/acs.jpcc.9b06890
J. Phys. Chem. C XXXX, XXX, XXX−XXX

For the PL experiments, an aqueous 0.6 M NaCl solution was prepared or demineralized water was used. Pure water has a specified pH of about 7; for the NaCl solution in water, the pH was found to be equal to 6.5. For acidification, the pH of the solutions was adjusted to a value of 3.3 using diluted HNO_3. Prior to each measurement, a fresh TiO_2 sample was placed in the fluorescence cuvette. The cuvette was filled with the respective solution and degassed with Ar for 30 min and sealed with a tight cuvette lid and laboratory sealing film.

PL measurements on a TiO_2 film in a methanol/acidified water solution (molar ratio of 1:1) show a faster PL decay compared to the pure pH 3.3 solution (see Figure S1). The observed faster decay is likely due to scavenging of surface-trapped holes with methanol reported earlier to occur in 300 ps.[55]

Similar photodynamics were observed for TiO_2 films prepared from water- and methanol-based suspensions (Figure S2), excluding an effect of possible residues of methanol from sample preparation on the PL dynamics. This result is in line with the earlier work, reporting an exchange of adsorbed methanol with H_2O, especially when the latter is in excess.[20] All further PL measurements were therefore performed on films prepared from suspension in methanol.

Time-Resolved PL Experiments. The output of a Fianium laser (FP-532-1-s, center wavelength 532 nm, pulse duration of 300 fs, 80.37 MHz repetition rate) was focused using a lens with 100 mm focal distance into a 3 mm thick β-BaB_2O_4 crystal (Newlight Photonics). The second harmonic UV signal generated was sent via three dichroic mirrors (Thorlabs, MBI-K04) and a FGUV11-UV filter (Thorlabs) to remove the residual 532 nm component and focused using a 50 mm focal distance quartz lens through the quartz window of the cuvette and the aqueous solution on the TiO_2 film. The PL was collected using two 2 in. diameter 50 mm focal length glass lenses and focused on the input of a spectrograph (Acton SP2300, Princeton Instruments, slit width set at 100 μm) using a grating with 50 lines/mm blazed at 600 nm. The output of the spectrograph was sent into a streak camera setup (Hamamatsu, C10910). The background signal from a photo-excited bare quartz substrate was verified to be negligible compared to the PL signal from the TiO_2 film. Prior to each series of time-resolved PL experiments, the spectral calibration was checked and adapted if necessary using a Hg/Ar calibration lamp (Oriel, LSP035). Spectral sensitivity correction of the PL spectra was performed using the difference between the measured and calibrated spectrum of a black body lamp (Ocean Optics, HL-2000). A possible contribution of trapping of emitted photons in the nanostructured TiO_2 network to the observed PL decay was excluded by the observation that exposure of the TiO_2 film to a fraction of the 532 nm output of the Fianium laser leads to significantly faster scattered signals (see Figure S3). Potential light-induced changes in time-resolved PL were excluded on the basis of similar PL intensity before and after data collection. For each experiment, a fresh TiO_2 sample was used, and all the experiments were performed in duplo . In a range of 4×10^{10} to 2×10^{11} photons/pulse cm^{-2}, the PL intensity scales approximately linearly with the incident UV intensity. The data presented here were recorded using an incident intensity of 1×10^{11} photons/pulse cm^{-2}. In addition, no intensity dependence of the PL decay was observed (see Figure S4).

The time windows covered were either 2 ns (i.e., time range 5) or 200 ps (i.e., time range 2). For the first, the slit width in front of the photocathode of the streak camera tube was set at 170 μm, yielding a time resolution of 30 ± 1 ps. To improve the time resolution at time range 2, the slit width in front of the photocathode was reduced to 20 μm, resulting in a time resolution of 10 ± 1 ps. Global analysis of the time-resolved PL data was performed using the open-source program Glotaran.[56] A parallel decay model with three pathways was found to accurately describe the spectrotemporal PL behavior. The values of τ_1, τ_2, and τ_3 were initially determined from the data recorded at time range 5. A more accurate value of τ_1 was subsequently determined from the data at time range 2, while keeping the values of τ_2 and τ_3 fixed. This iteration was repeated a number of times until the values of τ_1, τ_2, and τ_3 became stabilized, that is, changed less than the error.

RESULTS AND DISCUSSION

Figure 1 shows the scanning electron micrograph of the nanostructured TiO_2 thin films investigated. The individual

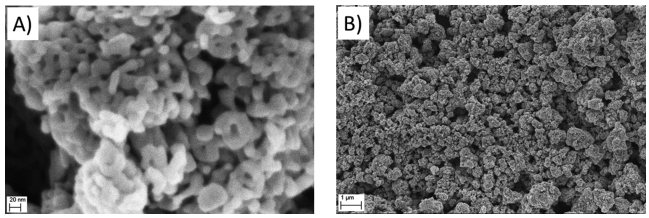

Figure 1. Scanning electron micrographs of the TiO_2 films studied with scale bars of 20 nm (A) and 1 μm (B).

TiO_2 particles have a size of ~20 nm (A), which form larger clusters of approximately a few 100 nm. The TiO_2 clusters adhere well to the quartz substrate resulting in a homogeneous film (B). The X-ray diffraction pattern (Figure S5) shows that the TiO_2 is in the anatase phase.

Figure 2A shows the PL spectra at 50, 250 ps, and 1 ns after 267 nm photoexcitation of a TiO_2 film in demineralized water degassed with Ar, showing a decay at a ps to ns time scale. Figure 2B shows the spectra for TiO_2 in similar aqueous media with 0.6 M NaCl added. The PL maximum shows a minor bathochromic shift in time from 491 nm (2.53 eV) to 494 nm (2.51 eV), in line with the value of ca. 2.5 eV for steady-state PL spectra.[11] The spectra are well described by two Gaussian functions, centered at 492 nm (2.52 eV, rms = 0.23 eV) and 636 nm (1.95 eV, rms = 0.10 eV), with the relative intensity of the PL band at 1.95 eV increasing in time after photoexcitation (see Figure S6 and Table S1). This trend is analogous to the slowing down in PL decay with decreasing photon energy both in the absence and presence of NaCl (see Figure S7 of the Supporting Information). At neutral conditions, the addition of NaCl does not have a significant effect on the PL spectra and decays. As the point of zero charge of TiO_2 is around 6,[52] this indicates that surface adsorption of Na^+ ions does not affect the PL, which is in agreement with insignificant effects of, for example, $NaNO_3$ on the photocatalytic efficiency.[51]

To facilitate surface adsorption of Cl^- ions and mimic changes in pH that could occur during photocatalytic reactions,[51] experiments have also been performed at mildly acidic conditions. Figure 2 includes the PL spectra at various times after photoexcitation of a TiO_2 film in pH 3.3 solution degassed with Ar, without (C) and with 0.6 M NaCl added

DOI: 10.1021/acs.jpcc.9b06890
J. Phys. Chem. C XXXX, XXX, XXX−XXX

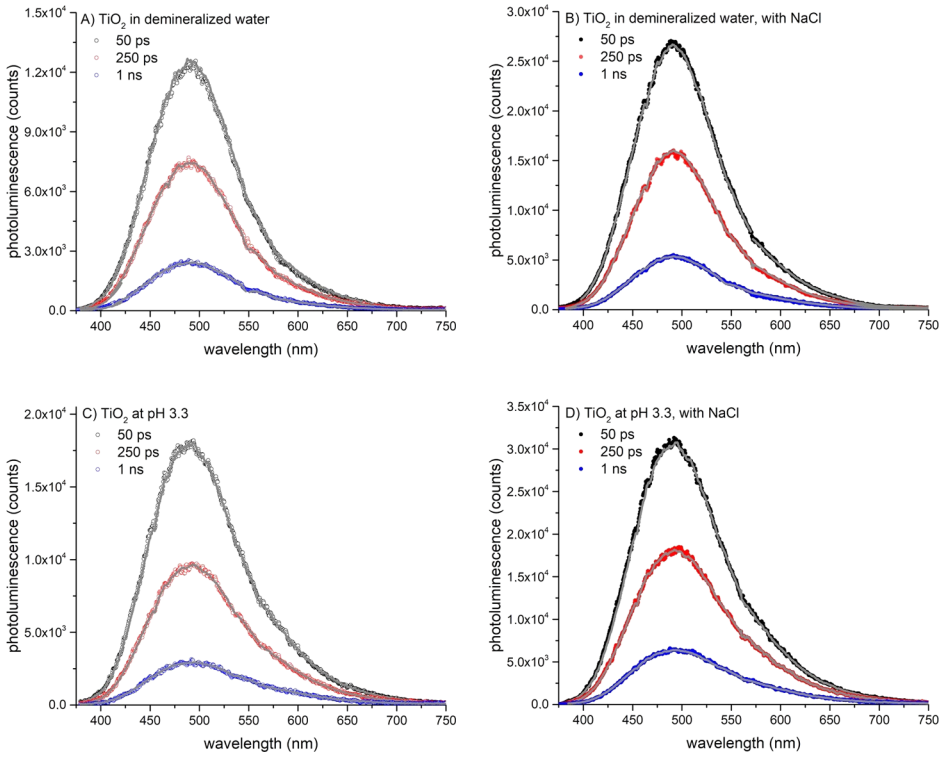

Figure 2. PL spectra at 50, 250 ps, and 1 ns after 267 nm photoexcitation, for TiO_2 films in demineralized water (A), demineralized water with 0.6 M NaCl added (B), in pH 3.3 solution (C), and in pH 3.3 solution with 0.6 M NaCl added (D). The solid lines are fits from global analysis using a parallel decay model with three components.

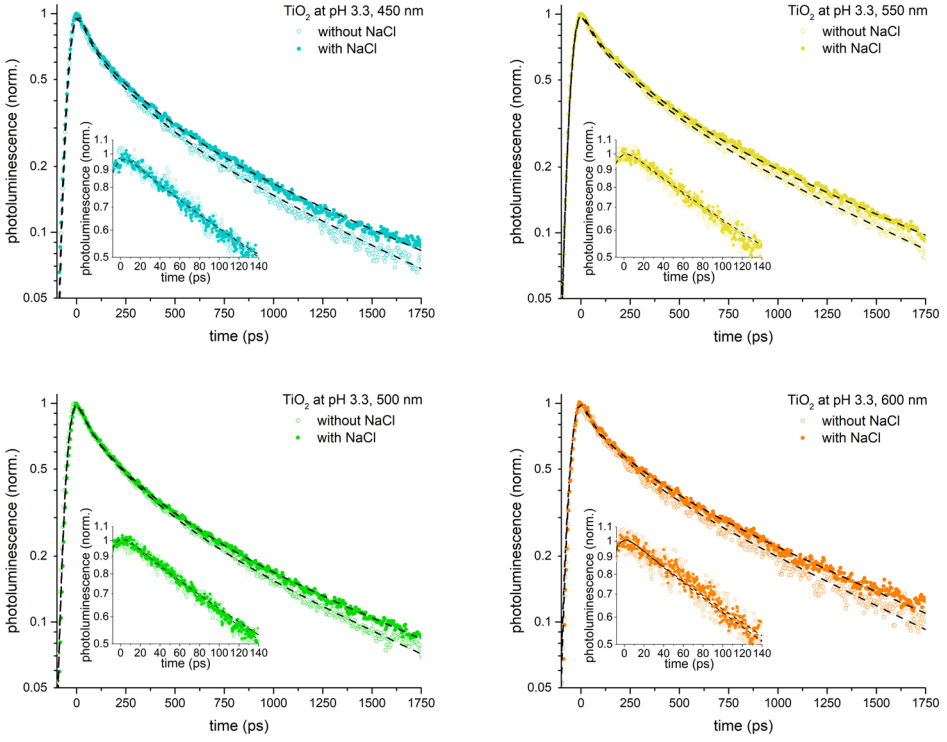

Figure 3. Normalized PL decays at various wavelengths of a TiO_2 film in pH 3.3 solution in the absence and presence of 0.6 M NaCl, at 267 nm excitation and using a 2 ns time window (time range 5), including fits from global analysis (dashed lines). The insets show the data and fits measured using a 200 ps time window (time range 2); note that better time resolution allows resolving faster initial decay.

(D). The spectra are well described by two Gaussian functions, one similar to neutral conditions at 492 nm (2.52 eV, rms = 0.23 eV) and one centered at 605 nm (2.05 eV, rms = 0.15 eV, Figure S8 and Table S2). Note that the latter band has blue-shifted relative to neutral conditions (1.95 eV) and has become relatively more intense (see also Tables S1 and S2 of the

DOI: 10.1021/acs.jpcc.9b06890
J. Phys. Chem. C XXXX, XXX, XXX−XXX

Supporting Information). On the contrary, the band at 2.52 eV is not affected by the change in pH. The intensity of the PL band centered at 2.05 eV relative to the band at 2.52 eV increases with time, analogous to the slowing down in PL decay with decreasing photon energy (Figure 3). In addition, at pH = 3.3, the addition of NaCl slows down the PL decay >500 ps, which will be discussed below. The surface/environment effect on the low energy PL band only (2.05 eV for pH 3.3, 1.95 eV for neutral conditions) and the effect of NaCl at pH 3.3 on the PL decay >500 ps indicate a correlation, in agreement with the slower PL decays at lower photon energies generally observed.

Figure 3 compares the normalized PL decays of the TiO_2 films in pH 3.3 solution at PL wavelengths of 450, 500, 550, and 600 nm in the absence and presence of 0.6 M NaCl, demonstrating a slower decay in the presence of NaCl. The main windows present data measured using a 2 ns time window, the insets using a time window of 200 ps. Across the entire PL spectrum, the signal fully develops within the instrumental response time, indicating that all the emitting species are formed in <10 ps. Note that the PL experiments have been performed in the linear regime, that is, the PL intensity scales linearly with the incident intensity and the normalized PL decays are independent of the incident intensity (see Experimental Methods and Figure S4). In all the cases, multi-exponential decay is observed, indicating multiple trapping and de-trapping of charge carriers.[6] The decays in the absence and presence of NaCl at similar wavelengths are identical until a few 100 ps but start to deviate significantly beyond with a slower decay for the TiO_2 film in a mildly acidic environment with NaCl present. As the PL signal has fully decayed at the next photo-excitation event (see Figure S9 of the Supporting Information), an artifact caused by a potential long-lived signal is ruled out. Moreover, the NaCl-induced effect on the PL decay exceeds the experimental noise by approximately 1 order of magnitude and is hence significant (see Figure S9 of the Supporting Information). Duplo experiments at pH = 3.3 (Figure S10) show an identical NaCl-induced effect on the PL decay dynamics.

The PL data could not be modeled adequately by an extended exponential function, derived from a random walk diffusion charge model and based on a distribution of transport and recombination rates.[47] Fits using a stretched exponential function have only been achieved with a wavelength-dependent shape factor (β) and lifetime (τ), see Figure S11. No global fit with one parameter set for the entire PL spectrotemporal behavior has been obtained. In particular a photophysical interpretation of the variation in β is not evident. However, global analysis shows that the spectrotemporal PL behavior is well described by a parallel model with three decay pathways. A parallel decay model instead of a sequential model for global analysis has been chosen because of the full development of the PL signal within the instrumental response time and the absence of a subsequent ingrowth. Note that this model is likely a simplification of the reality; however, it describes all PL behavior observed here adequately. The resulting fits are included in Figures 2 and 3. Table 1 presents the PL lifetimes and the relative change in lifetime induced by the addition of NaCl. Our values are reasonably close to the PL lifetimes found by Dozzi et al. of 25, 269 ps, and 4.4 ns, based on analysis of a narrow wavelength range[45] instead of the present global analysis of the entire PL spectrum and its development in time.

Table 1. PL Lifetimes from Global Analysis Using a Parallel Model with three Decays[a]

conditions	τ_1 (ps)	τ_2 (ps)	τ_3 (ps)
demineralized water	42 ± 1	225 ± 2	1056 ± 5
demineralized water, with NaCl	48 ± 2 [14 ± 7%]*	238 ± 2 [6 ± 2%]#	1042 ± 4 [−1±1%]
pH = 3.3, without NaCl	46 ± 2	257 ± 1	1048 ± 2
pH = 3.3, with NaCl	47 ± 1 [2 ± 6%]	269 ± 1 [4 ± 1%]	1167 ± 2 [11 ± 0%]
nature PL	bulk	intermediate behavior	effect of surface adsorption

[a]Between square brackets is the relative change in lifetime induced by NaCl. Note that the absolute difference is only 6 ± 3 ps (*) and 13 ± 4 ps (#), in agreement with the similar PL decays at neutral conditions in the absence and presence of NaCl.

At neutral conditions, the effect of NaCl addition on all lifetimes is within the experimental error, in agreement with the similar PL decays (Figure S7). However, at pH = 3.3, the effect of NaCl addition on, in particular, τ_3 exceeds the experimental error, with a relative change of 11 ± 0%. The impact on τ_2 is barely significant and any influence on τ_1 is absent. These effects indicate an effect of surface adsorbates on τ_3. Note that this does not necessarily imply that τ_3 is purely governed by recombination processes altered by surface termination, as PL lifetime is the result of all decay processes available. Because the point of zero charge of TiO_2[52] is around 6, the effect of NaCl addition at pH = 3.3 on τ_3 is likely due to surface adsorption of Cl^- ions. This process is suppressed at neutral conditions because of the negative surface charge, while an effect of Na^+ adsorption on the PL decay is absent as discussed above. The value of τ_1 is unaffected by surface termination and is likely associated to electron−hole recombination in the bulk of the nanoparticle. A significant influence of light trapping inside the nanostructured TiO_2 network on the observed PL dynamics is excluded because exposure to a fraction of 532 nm 300 fs pulses (used for second harmonic generation of the UV light used for photoexcitation) gives significantly faster decays (Figure S3). The origin of τ_2 is unclear. Considering the gradual broadening of the PL spectrum in time, we cautiously assign τ_2 to a decay process with intermediate behavior between bulk recombination (τ_1) and recombination sensitive to surface termination (τ_3).

Figure 4 shows the normalized DAS obtained from global analysis of the PL data at pH 3.3,[50] that is, DAS1 decays with τ_1, DAS2 with τ_2, and DAS3 with τ_3, including fits based on the sum of two Gaussian functions (parameters in Table 2). Relative to DAS1, DAS2 and especially DAS3 are significantly broader at the low energy side of the spectrum. The normalized spectra are similar in the absence and in the presence of NaCl, however, τ_3 differs. The PL maximum shows a weak bathochromic shift in time from 489 nm (2.54 eV) for DAS1 to 494 nm (2.51 eV) for DAS3. Pallotti et al. assigned PL around 2.5 eV to surface recombination of mobile electrons with trapped holes.[11] The effect of NaCl addition at acidic conditions on mainly τ_3 enables to advance this model, strongly indicating that PL originates from a time-dependent mix of processes independent (at early times) and influenced by surface adsorbates (>500 ps). These processes also likely cause the bathochromic shift and the relatively more intense PL band at 2.05 eV for DAS3.

DOI: 10.1021/acs.jpcc.9b06890
J. Phys. Chem. C XXXX, XXX, XXX−XXX

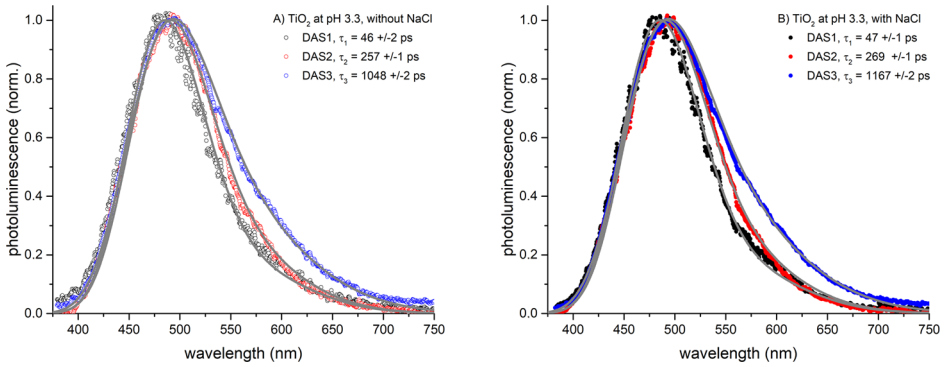

Figure 4. Normalized DAS and corresponding decay times of TiO_2 film in pH 3.3 solution in the absence (A) and presence of 0.6 M NaCl (B), including the sum of two Gaussian functions (solid gray curves, parameters in Table 2).

Table 2. Parameters of the Gaussian Functions Used for Spectral Deconvolution of the DAS Spectra

	TiO_2 at pH 3.3, without NaCl			TiO_2 at pH 3.3, with 0.6 M NaCl		
spectrum	Gauss 1 (eV)	Gauss 2 (eV)	amplitude ratio	Gauss 1 (eV)	Gauss 2 (eV)	amplitude ratio
DAS1	2.54	2.05	0.07	2.54	2.05	0.07
	rms = 0.21	rms = 0.15		rms = 0.21	rms = 0.15	
DAS2	2.52	2.05	0.07	2.52	2.05	0.07
	rms = 0.22	rms = 0.15		rms = 0.22	rms = 0.15	
DAS3	2.51	2.05	0.12	2.51	2.05	0.12
	rms = 0.24	rms = 0.18		rms = 0.24	rms = 0.18	

The observed effects could have several origins. Changes in band bending is known to alter, in particular, the PL yield[40,41] and may be responsible for the observed effect of Cl^- adsorption on the PL decay >500 ps. For small TiO_2 nanoparticles (radius 3.8−12 nm), band bending is likely minor or even absent,[41] however, clustering of nanoparticles into a nanoporous film may induce band bending. In addition, UV excitation has been reported to reduce band bending and lead to a flat band structure.[40] Cl^- adsorption may increase upward band bending and reduce the probability of electron−hole recombination. The structure of the surface may also influence rate constants for radiative and nonradiative recombination. The increasing effect of Cl^- adsorption on the PL in time observed here indicates motion of photo-induced species from the bulk toward a potential depletion layer and/or the surface of the nanoparticle. Such directional motion can explain the slower PL decay at lower photon energy observed in the all cases here and the pH-induced shift of the low energy band from 1.95 eV at neutral conditions to 2.05 eV at pH = 3.3, while the position of the band centered at 2.52 eV is unaffected by this change in pH and only shows a weak bathochromic shift of ca. 0.03 eV with time.

The hot charge carriers initially generated by photo-excitation likely thermalize at an ultrafast time scale by charge−phonon coupling. Chergui et al. recently reported an electron cooling time of <50 fs.[21] Femtosecond transient absorption studies have shown that holes become trapped at surface sites in ∼200 fs, followed by >100 ps relaxation into deeper traps.[57] For electrons, the situation is likely more complex, with some electrons trapped at the surface at a similar ∼200 fs time scale and other electrons occupying shallow traps close to the CB.[13] Hence, during photoexcitation with the ca. 300 fs 267 nm laser pulse, at least three species are likely to be formed: (1) bulk electrons in the CB or a shallow trap state, (2) surface-trapped electrons, and (3) surface-trapped holes. In addition, some holes may be trapped in the bulk of the TiO_2 nanoparticle.

It should be noted that the PL decays observed here are rather similar to the transient absorption decay at 1200 nm probing electron recombination,[14] suggesting that the PL dynamics and the broadening in the PL spectrum in time are mainly driven by motion of electrons rather than holes, although some contribution of the latter cannot be excluded. This assignment is in line with theoretical work[32,58] and consistent with an electron diffusion constant for nano-structured TiO_2 of ca. 2×10^{-5} cm^2/s,[59] indicating a ∼1−2 ns random walk diffusion time from the bulk of the TiO_2 nanoparticle in the direction of the depletion layer/surface.

The ps−ns PL decay can explain the strong PL quenching when increasing the temperature and the shift in PL from ca. 2.5 eV (496 nm) at 300 K to ca. 2.3 eV (539 nm) at 100 K.[25] The PL at low temperature has been assigned to radiative decay of STEs stabilized by lattice relaxation.[2,25,60] An exciton in anatase TiO_2 is likely to be of intermediate character between a Wannier-Mott and a Frenkel exciton.[61] Microwave conductivity experiments have shown that interaction of mobile electrons with trapped holes could lead to the generation of long-lived STEs at a sub-ns time scale, formed with a quantum yield of 65% at 100 K and <5% at 300 K.[17] The temperature-independent STE lifetime of 3.3 ± 0.2 μs[17] agrees reasonably well with the PL lifetime at 2 K of 1.5−2.0 μs,[62] suggesting that PL at low temperature is at least partially due to STE decay. The low STE yield at 300 K[17] shows that at room temperature, sufficient phonon energy is available for STE detrapping. The resulting mobile electrons could rapidly recombine radiatively or nonradiatively with trapped holes via one of the ps−ns pathways deduced in the present work, explaining the thermally deactivated PL.[2,25]

Figure 5 presents a photophysical model for the time-dependent PL spectrum of nanostructured anatase TiO_2 in aqueous media, explaining the observed bathochromic shift

DOI: 10.1021/acs.jpcc.9b06890
J. Phys. Chem. C XXXX, XXX, XXX−XXX

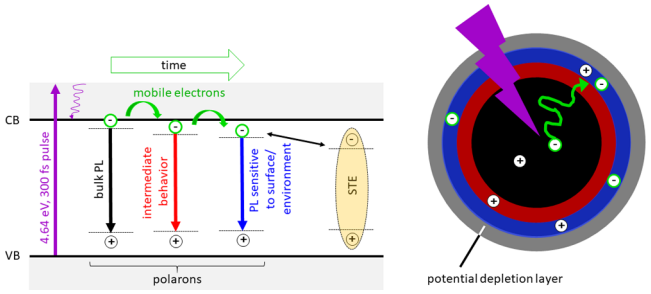

Figure 5. Model discriminating between PL due to bulk recombination and PL sensitive to surface termination, with the contribution of the latter increasing with time because of diffusion of electrons from the bulk in the direction of a potential depletion layer/the surface and their recombination with immobile hole polarons. Mobile electrons may also be formed by phonon-assisted detrapping of STEs, VB = valence band, CB = conduction band.

and pH-dependent broadening at the low energy side of the spectrum in time. We show by global analysis that the ps–ns PL processes can be adequately described by a parallel model with three decay components, with the contribution of processes affected by surface termination increasing with time. The ~46 ps decay is indicative of recombination via an Auger mechanism reported earlier in transient absorption studies.[63] However, as the PL decay is insensitive to the number of incident photons (Figure S4B), such mechanism is excluded. As the presence of NaCl does not affect τ_1, this recombination process likely occurs in the bulk of the TiO_2 nanoparticle. Considering that the probability of recombination decreases with trapping because of a decrease in charge mobility, this process is most likely related to mobile electrons in the CB or a shallow trap interacting with trapped holes in the bulk. With progression in time after photoexcitation, mobile electrons could move from the bulk in the direction of a potential depletion layer and the surface. This assignment agrees with electronic structure calculations, indicating for the bulk shallow electron traps at Ti^{4+} sites and deep hole traps at O_2^- sites, while for the (101) surface, deep electron and deep hole traps ascribed to under-coordinated Ti_{5c}^{3+} and O_{2c}^- sites were found.[32] The trapping process was observed to lead to a strong elongation in the bond length, and de-trapping from these states is unlikely at ps–ns time scales. It should be noted that the nature and distribution of trap states is likely facet-dependent, as shown recently by density functional theory.[58] The origin of the ~260 ps component barely influenced by NaCl is unclear. Considering the gradual broadening of the PL spectrum at the low energy side in time (Figure 4), we cautiously assign τ_2 to a decay process with intermediate behavior between bulk recombination (τ_1) and recombination sensitive to surface adsorption (τ_3). The value of τ_3 of ca. 1 ns affected by surface adsorption of Cl^- ions is likely due to recombination of relatively mobile electrons, possibly formed by detrapping of STEs, with immobile holes in a deep trap close to or within the depletion layer or at the surface, probably an O_{2c}^- site.[32] Cl^- adsorption may increase upward band bending, thereby reducing the probability of electron–hole recombination and increasing τ_3. The structure of the surface may also influence rate constants for radiative and nonradiative recombination. The negative effect of chloride on photocatalytic rates[51] (in acidic conditions) is likely due to modifications of the surface caused by the adsorbents, leading to the observed change in τ_3. Diffusion in the direction of the depletion layer/surface is vital for photocatalytic reactions and likely plays an important role in the photocatalytic activity of nanostructured anatase TiO_2.

CONCLUSIONS

In the present work, we show that the PL spectrum of commercial nanostructured anatase TiO_2 thin films in various aqueous media closely resembling photocatalytic conditions is time-dependent, with a minor bathochromic shift and a broadening at the low energy side of the spectrum in time. We demonstrate the potential of global analysis to develop mechanistic insight and show that the development of the PL spectrum in time is due to an increasing contribution of processes influenced by surface adsorption relative to bulk processes. This trend can be assigned to recombination of mobile electrons populating the CB or shallow traps with immobile hole polarons in deep traps and the motion of electrons from the nanoparticle bulk in the direction of the depletion layer/surface in ca. 1 ns.

The observed directional diffusion is likely to have major consequences for photocatalytic applications. Control of the directional motion of electrons and suppression of surface charge recombination via surface engineering show promise to further increase the photocatalytic activity. Future research in our group is underway and focused on understanding charge carrier behavior of other photocatalytic materials as well and optimizing such photocatalysts with the insights obtained.

ASSOCIATED CONTENT

Supporting Information

The Supporting Information is available free of charge on the ACS Publications website at DOI: 10.1021/acs.jpcc.9b06890.

X-ray diffraction pattern TiO_2; PL decays in the presence and absence of methanol, for TiO_2 films in demineralized water in the absence and presence of 0.6 M NaCl; scattering dynamics in nanostructured TiO_2 film; photo-excitation intensity dependencies; spectral deconvolutions of PL spectra at various time points after photoexcitation; and DUPLO experiments addressing the reproducibility of the NaCl-induced effect observed at mildly acidic conditions and fits to PL decays using a stretched exponential decay function (PDF)

AUTHOR INFORMATION

Corresponding Author

*E-mail: j.m.huijser@utwente.nl.

ORCID

Bastian T. Mei: 0000-0002-3973-9254
Guido Mul: 0000-0001-5898-6384
Annemarie Huijser: 0000-0003-0381-6155

Author Contributions

R.B. and K.W. have contributed equally. The manuscript was written through contributions of all the authors. All the authors have given approval to the final version of the manuscript.

Notes

The authors declare no competing financial interest.

ACKNOWLEDGMENTS

Alyssa van Duijne is acknowledged for preliminary studies.

DOI: 10.1021/acs.jpcc.9b06890
J. Phys. Chem. C XXXX, XXX, XXX–XXX

■ ABBREVIATIONS

CB, conduction band; DAS, decay-associated spectrum; PL, photoluminescence; rms, root mean square; SEM, scanning electron microscopy; STE, self-trapped exciton; VB, valence band

■ REFERENCES

(1) Nakata, K.; Fujishima, A. TiO_2 photocatalysis: Design and applications. *J. Photochem. Photobiol., C* **2012**, *13*, 169−189.
(2) Gallart, M.; Cottineau, T.; Hönerlage, B.; Keller, V.; Keller, N.; Gilliot, P. Temperature dependent photoluminescence of anatase and rutile TiO_2 single crystals: Polaron and self-trapped exciton formation. *J. Appl. Phys.* **2018**, *124*, 133104.
(3) Pelaez, M.; Nolan, N. T.; Pillai, S. C.; Seery, M. K.; Falaras, P.; Kontos, A. G.; Dunlop, P. S. M.; Hamilton, J. W. J.; Byrne, J. A.; O'Shea, K.; et al. A review on the visible light active titanium dioxide photocatalysts for environmental applications. *Appl. Catal., B* **2012**, *125*, 331−349.
(4) Gupta, S. M.; Tripathi, M. A review of TiO_2 nanoparticles. *Chin. Sci. Bull.* **2011**, *56*, 1639.
(5) Di Paola, A.; Bellardita, M.; Palmisano, L. Brookite, the Least Known TiO_2 Photocatalyst. *Catalysts* **2013**, *3*, 36−73.
(6) Yamada, Y.; Kanemitsu, Y. Determination of electron and hole lifetimes of rutile and anatase TiO_2 single crystals. *Appl. Phys. Lett.* **2012**, *101*, 133907.
(7) Schindler, K. M.; Kunst, M. Charge-carrier dynamics in titania powders. *J. Phys. Chem.* **1990**, *94*, 8222−8226.
(8) Knorr, F. J.; Zhang, D.; McHale, J. L. Influence of $TiCl_4$ Treatment on Surface Defect Photoluminescence in Pure and Mixed-Phase Nanocrystalline TiO_2. *Langmuir* **2007**, *23*, 8686−8690.
(9) Knorr, F. J.; Mercado, C. C.; McHale, J. L. Trap-State Distributions and Carrier Transport in Pure and Mixed-Phase TiO_2: Influence of Contacting Solvent and Interphasial Electron Transfer. *J. Phys. Chem. C* **2008**, *112*, 12786−12794.
(10) Mercado, C. C.; Knorr, F. J.; McHale, J. L.; Usmani, S. M.; Ichimura, A. S.; Saraf, L. V. Location of Hole and Electron Traps on Nanocrystalline Anatase TiO_2. *J. Phys. Chem. C* **2012**, *116*, 10796−10804.
(11) Pallotti, D. K.; Passoni, L.; Maddalena, P.; Di Fonzo, F.; Lettieri, S. Photoluminescence Mechanisms in Anatase and Rutile TiO_2. *J. Phys. Chem. C* **2017**, *121*, 9011−9021.
(12) Mascaretti, L.; Russo, V.; Zoppellaro, G.; Lucotti, A.; Casari, C. S.; Kment, Š.; Naldoni, A.; Li Bassi, A. Excitation Wavelength- and Medium-Dependent Photoluminescence of Reduced Nanostructured TiO_2 Films. *J. Phys. Chem. C* **2019**, *123*, 11292−11303.
(13) Tamaki, Y.; Furube, A.; Murai, M.; Hara, K.; Katoh, R.; Tachiya, M. Dynamics of efficient electron−hole separation in TiO_2 nanoparticles revealed by femtosecond transient absorption spectroscopy under the weak-excitation condition. *Phys. Chem. Chem. Phys.* **2007**, *9*, 1453−1460.
(14) Sachs, M.; Pastor, E.; Kafizas, A.; Durrant, J. R. Evaluation of Surface State Mediated Charge Recombination in Anatase and Rutile TiO_2. *J. Phys. Chem. Lett.* **2016**, *7*, 3742−3746.
(15) Bahnemann, D. W.; Hilgendorff, M.; Memming, R. Charge Carrier Dynamics at TiO_2 Particles: Reactivity of Free and Trapped Holes. *J. Phys. Chem. B* **1997**, *101*, 4265−4275.
(16) Cowan, A. J.; Tang, J.; Leng, W.; Durrant, J. R.; Klug, D. R. Water Splitting by Nanocrystalline TiO_2 in a Complete Photoelectrochemical Cell Exhibits Efficiencies Limited by Charge Recombination. *J. Phys. Chem. C* **2010**, *114*, 4208−4214.
(17) Fravventura, M. C.; Siebbeles, L. D. A.; Savenije, T. J. Mechanisms of Photogeneration and Relaxation of Excitons and Mobile Carriers in Anatase TiO_2. *J. Phys. Chem. C* **2014**, *118*, 7337−7343.
(18) Savenije, T. J.; Huijser, A.; Vermeulen, M. J. W.; Katoh, R. Charge carrier dynamics in TiO_2 nanoparticles at various temperatures. *Chem. Phys. Lett.* **2008**, *461*, 93−96.
(19) Katoh, R.; Huijser, A.; Hara, K.; Savenije, T. J.; Siebbeles, L. D. A. Effect of the Particle Size on the Electron Injection Efficiency in Dye-Sensitized Nanocrystalline TiO_2 Films Studied by Time-Resolved Microwave Conductivity (TRMC) Measurements. *J. Phys. Chem. C* **2007**, *111*, 10741−10746.
(20) Wang, C.-y.; Groenzin, H.; Shultz, M. J. Comparative Study of Acetic Acid, Methanol, and Water Adsorbed on Anatase TiO_2 Probed by Sum Frequency Generation Spectroscopy. *J. Am. Chem. Soc.* **2005**, *127*, 9736−9744.
(21) Baldini, E.; Palmieri, T.; Pomarico, E.; Auböck, G.; Chergui, M. Clocking the Ultrafast Electron Cooling in Anatase Titanium Dioxide Nanoparticles. *ACS Photonics* **2018**, *5*, 1241−1249.
(22) Zhang, J.; Chen, X.; Shen, Y.; Li, Y.; Hu, Z.; Chu, J. Synthesis, surface morphology, and photoluminescence properties of anatase iron-doped titanium dioxide nano-crystalline films. *Phys. Chem. Chem. Phys.* **2011**, *13*, 13096−13105.
(23) Cavigli, L.; Bogani, F.; Vinattieri, A.; Faso, V.; Baldi, G. Volume versus surface-mediated recombination in anatase TiO_2 nanoparticles. *J. Appl. Phys.* **2009**, *106*, 053516.
(24) Schneider, J.; Matsuoka, M.; Takeuchi, M.; Zhang, J.; Horiuchi, Y.; Anpo, M.; Bahnemann, D. W. Understanding TiO_2 Photocatalysis: Mechanisms and Materials. *Chem. Rev.* **2014**, *114*, 9919−9986.
(25) Tang, H.; Berger, H.; Schmid, P. E.; Lévy, F.; Burri, G. Photoluminescence in TiO_2 anatase single crystals. *Solid State Commun.* **1993**, *87*, 847−850.
(26) Tang, H.; Lévy, F.; Berger, H.; Schmid, P. E. Urbach tail of anatase TiO_2. *Phys. Rev. B: Condens. Matter Mater. Phys.* **1995**, *52*, 7771−7774.
(27) Mercado, C.; Seeley, Z.; Bandyopadhyay, A.; Bose, S.; McHale, J. L. Photoluminescence of Dense Nanocrystalline Titanium Dioxide Thin Films: Effect of Doping and Thickness and Relation to Gas Sensing. *ACS Appl. Mater. Interfaces* **2011**, *3*, 2281−2288.
(28) Pallotti, D. K.; Orabona, E.; Amoruso, S.; Aruta, C.; Bruzzese, R.; Chiarella, F.; Tuzi, S.; Maddalena, P.; Lettieri, S. Multi-band photoluminescence in TiO_2 nanoparticles-assembled films produced by femtosecond pulsed laser deposition. *J. Appl. Phys.* **2013**, *114*, 043503.
(29) Wang, X.; Feng, Z.; Shi, J.; Jia, G.; Shen, S.; Zhou, J.; Li, C. Trap states and carrier dynamics of TiO_2 studied by photoluminescence spectroscopy under weak excitation condition. *Phys. Chem. Chem. Phys.* **2010**, *12*, 7083−7090.
(30) Iijima, K.; Goto, M.; Enomoto, S.; Kunugita, H.; Ema, K.; Tsukamoto, M.; Ichikawa, N.; Sakama, H. Influence of oxygen vacancies on optical properties of anatase TiO_2 thin films. *J. Lumin.* **2008**, *128*, 911−913.
(31) Abazović, N. D.; Čomor, M. I.; Dramićanin, M. D.; Jovanović, D. J.; Ahrenkiel, S. P.; Nedeljković, J. M. Photoluminescence of Anatase and Rutile TiO_2 Particles. *J. Phys. Chem. B* **2006**, *110*, 25366−25370.
(32) Di Valentin, C.; Selloni, A. Bulk and Surface Polarons in Photoexcited Anatase TiO2. *J. Phys. Chem. Lett.* **2011**, *2*, 2223−2228.
(33) Deskins, N. A.; Dupuis, M. Electron transport via polaron hopping in bulk TiO2: A density functional theory characterization. *Phys. Rev. B: Condens. Matter Mater. Phys.* **2007**, *75*, 195212.
(34) Deskins, N. A.; Dupuis, M. Intrinsic Hole Migration Rates in TiO2 from Density Functional Theory. *J. Phys. Chem. C* **2009**, *113*, 346−358.
(35) Deskins, N. A.; Rousseau, R.; Dupuis, M. Localized Electronic States from Surface Hydroxyls and Polarons in TiO2(110). *J. Phys. Chem. C* **2009**, *113*, 14583−14586.
(36) De Lile, J. R.; Kang, S. G.; Son, Y.-A.; Lee, S. G. Investigating Polaron Formation in Anatase and Brookite TiO2 by Density Functional Theory with Hybrid-Functional and DFT plus U Methods. *ACS Omega* **2019**, *4*, 8056−8064.
(37) Emeline, A. V.; Ryabchuk, V. K.; Serpone, N. Dogmas and Misconceptions in Heterogeneous Photocatalysis. Some Enlightened Reflections. *J. Phys. Chem. B* **2005**, *109*, 18515−18521.
(38) Saleh, B. E. A.; Teich, M. C. *Fundamentals of Photonics*, 2nd ed.; John Wiley & Sons, Inc.: Hoboken, New Jersey, 2007.

DOI: 10.1021/acs.jpcc.9b06890
J. Phys. Chem. C XXXX, XXX, XXX−XXX

(39) Mercado, C. C.; Knorr, F. J.; McHale, J. L. Observation of Charge Transport in Single Titanium Dioxide Nanotubes by Micro-Photoluminescence Imaging and Spectroscopy. *ACS Nano* **2012**, *6*, 7270−7280.
(40) Stevanovic, A.; Büttner, M.; Zhang, Z.; Yates, J. T. Photoluminescence of TiO2: Effect of UV Light and Adsorbed Molecules on Surface Band Structure. *J. Am. Chem. Soc.* **2012**, *134*, 324−332.
(41) Zhang, Z.; Yates, J. T. Band Bending in Semiconductors: Chemical and Physical Consequences at Surfaces and Interfaces. *Chem. Rev.* **2012**, *112*, 5520−5551.
(42) Jung, K. Y.; Park, S. B.; Anpo, M. Photoluminescence and photoactivity of titania particles prepared by the sol−gel technique: effect of calcination temperature. *J. Photochem. Photobiol., A* **2005**, *170*, 247−252.
(43) Shi, J.; Chen, J.; Feng, Z.; Chen, T.; Lian, Y.; Wang, X.; Li, C. Photoluminescence Characteristics of TiO_2 and Their Relationship to the Photoassisted Reaction of Water/Methanol Mixture. *J. Phys. Chem. C* **2007**, *111*, 693−699.
(44) Sanjinés, R.; Tang, H.; Berger, H.; Gozzo, F.; Margaritondo, G.; Lévy, F. Electronic structure of anatase TiO_2 oxide. *J. Appl. Phys.* **1994**, *75*, 2945−2951.
(45) Dozzi, M. V.; D'Andrea, C.; Ohtani, B.; Valentini, G.; Selli, E. Fluorine-Doped TiO_2 Materials: Photocatalytic Activity vs Time-Resolved Photoluminescence. *J. Phys. Chem. C* **2013**, *117*, 25586−25595.
(46) Watanabe, M.; Hayashi, T. Time-resolved study of self-trapped exciton luminescence in anatase TiO_2 under two-photon excitation. *J. Lumin.* **2005**, *112*, 88−91.
(47) Fujihara, K.; Izumi, S.; Ohno, T.; Matsumura, M. Time-resolved photoluminescence of particulate TiO_2 photocatalysts suspended in aqueous solutions. *J. Photochem. Photobiol., A* **2000**, *132*, 99−104.
(48) Lefebvre, O.; Moletta, R. Treatment of organic pollution in industrial saline wastewater: A literature review. *Water Res.* **2006**, *40*, 3671−3682.
(49) Azevedo, E. B.; Neto, F. R. d. A.; Dezotti, M. TiO2-photocatalyzed degradation of phenol in saline media: lumped kinetics, intermediates, and acute toxicity. *Appl. Catal., B* **2004**, *54*, 165−173.
(50) van Stokkum, I. H. M.; Larsen, D. S.; van Grondelle, R. Global and target analysis of time-resolved spectra. *Biochim. Biophys. Acta, Bioenerg.* **2004**, *1657*, 82−104.
(51) Brüninghoff, R.; van Duijne, A. K.; Braakhuis, L.; Saha, P.; Jeremiasse, A. W.; Mei, B.; Mul, G. A comparative analysis of photocatalytic and electrochemical degradation of 4-Ethylphenol in saline conditions. *Environ. Sci. Technol.* **2019**, *53*, 8725−8735.
(52) Kosmulski, M. The significance of the difference in the point of zero charge between rutile and anatase. *Adv. Colloid Interface Sci.* **2002**, *99*, 255−264.
(53) Carneiro, J. T.; Almeida, A. R.; Moulijn, J. A.; Mul, G. Cyclohexane selective photocatalytic oxidation by anatase TiO_2: influence of particle size and crystallinity. *Phys. Chem. Chem. Phys.* **2010**, *12*, 2744−2750.
(54) Carneiro, J. T.; Savenije, T. J.; Moulijn, J. A.; Mul, G. Toward a Physically Sound Structure-Activity Relationship of TiO2-Based Photocatalysts. *J. Phys. Chem. C* **2010**, *114*, 327−332.
(55) Tamaki, Y.; Furube, A.; Murai, M.; Hara, K.; Katoh, R.; Tachiya, M. Direct observation of reactive trapped holes in TiO_2 undergoing photocatalytic oxidation of adsorbed alcohols: Evaluation of the reaction rates and yields. *J. Am. Chem. Soc.* **2006**, *128*, 416−417.
(56) Snellenburg, J. J.; Laptenok, S. P.; Seger, R.; Mullen, K. M.; van Stokkum, I. H. M. Glotaran: A Java-Based Graphical User Interface for the R Package TIMP. *J. Stat. Softw.* **2012**, *49*, 1−22.
(57) Tamaki, Y.; Furube, A.; Katoh, R.; Murai, M.; Hara, K.; Arakawa, H.; Tachiya, M. Trapping dynamics of electrons and holes in a nanocrystalline TiO_2 film revealed by femtosecond visible/near-infrared transient absorption spectroscopy. *Cron. Chim.* **2006**, *9*, 268−274.
(58) Carey, J. J.; McKenna, K. P. Does Polaronic Self-Trapping Occur at Anatase TiO_2 Surfaces? *J. Phys. Chem. C* **2018**, *122*, 27540−27553.
(59) Kopidakis, N.; Benkstein, K. D.; van de Lagemaat, J.; Frank, A. J.; Yuan, Q.; Schiff, E. A. Temperature dependence of the electron diffusion coefficient in electrolyte-filled TiO_2 nanoparticle films: Evidence against multiple trapping in exponential conduction-band tails. *Phys. Rev. B: Condens. Matter Mater. Phys.* **2006**, *73*, 045326.
(60) Saini, C. P.; Barman, A.; Banerjee, D.; Grynko, O.; Prucnal, S.; Gupta, M.; Phase, D. M.; Sinha, A. K.; Kanjilal, D.; Skorupa, W.; et al. Impact of Self-Trapped Excitons on Blue Photoluminescence in TiO_2 Nanorods on Chemically Etched Si Pyramids. *J. Phys. Chem. C* **2017**, *121*, 11448−11454.
(61) Baldini, E.; Chiodo, L.; Dominguez, A.; Palummo, M.; Moser, S.; Yazdi-Rizi, M.; Aubock, G.; Mallett, B. P. P.; Berger, H.; Magrez, A.; et al. Strongly bound excitons in anatase TiO_2 single crystals and nanoparticles. *Nat. Commun.* **2017**, *8*, 13.
(62) Watanabe, M.; Sasaki, S.; Hayashi, T. Time-resolved study of photoluminescence in anatase TiO_2. *J. Lumin.* **2000**, *87−89*, 1234−1236.
(63) Matsuzaki, H.; Matsui, Y.; Uchida, R.; Yada, H.; Terashige, T.; Li, B. S.; Sawa, A.; Kawasaki, M.; Tokura, Y.; Okamoto, H. Photocarrier dynamics in anatase TiO_2 investigated by pump-probe absorption spectroscopy. *J. Appl. Phys.* **2014**, *115*, 053514.

DOI: 10.1021/acs.jpcc.9b06890
J. Phys. Chem. C XXXX, XXX, XXX−XXX